Observation of the "Dark Exciton" in CdSe Quantum Dots

M. Nirmal, D. J. Norris, M. Kuno, and M. G. Bawendi
Massachusetts Institute of Technology, 77 Massachusetts Avenue, Cambridge, Massachusetts 02139

Al. L. Efros and M. Rosen
Beam Theory Section, Naval Research Laboratory, Washington, D.C. 20375
(Received 30 May 1995)

We use external magnetic fields to identify the band edge emitting state in CdSe quantum dots. The field dependence of emission decays and LO phonon spectra show the importance of exciton spin dynamics in the recombination mechanism. To interpret our results we calculate the band edge exciton structure, including the effects of the electron-hole exchange interaction and a nonspherical shape. The exchange term, negligible in the bulk, is strongly enhanced by quantum confinement and allows the observation of an optically passive "dark" excitonic state.

PACS numbers: 73.20.Dx, 63.20.Kr, 71.70.Ej, 71.70.Gm

Semiconductor nanocrystallites (or quantum dots) with dimensions smaller than the bulk exciton Bohr radius (a_B) exhibit discrete electronic states due to the three-dimensional confinement of the electron and hole [1,2]. This behavior is clearly evident in II-VI quantum dots (QDs), such as CdSe. While the absorption spectra of these dots are now fairly well understood [3,4], the nature of the emitting state remains controversial. This issue is complicated by the fact that the luminescence properties are highly dependent on sample preparation methods. The emission spectrum of many samples is dominated by "deep trap" emission, strongly redshifted from the band edge. However, new fabrication methods [5] yield dots which emit with high quantum yield (~0.1 to 0.9 at 10 K) at the band edge. Even these high quality samples exhibit unusually long radiative lifetimes ($\tau_R \sim 1$ μs at 10 K) [6] relative to the bulk exciton recombination time ($\tau_R \sim$ 1 ns) [7]. Since these radiative rates were expected to be comparable, band edge emission in II-VI QDs was rationalized as a "surface effect" and assigned to the recombination of weakly overlapping, surface-localized carriers [6,8]. In this Letter, however, we present new magnetic field data which now implicate exciton spin dynamics in the recombination mechanism. While QD models have largely neglected the effects of the electron-hole exchange interaction, we demonstrate that in CdSe this term, enhanced by quantum confinement, strongly modifies the band edge exciton structure [9,10]. Exciton thermalization to the lowest QD state, which is optically forbidden ("dark"), quantitatively explains the long lived emission, the luminescence Stokes shift, and the magnetic field dependence.

To determine the band edge exciton structure for CdSe QDs, we extend effective mass models used previously to describe their absorption spectra [3,4]. For spherical dots, the lowest state ($1S_{3/2}1S_e$) is eightfold degenerate in the spherical band approximation [3]. However, anisotropy in the internal crystal structure and/or shape of the dots lifts this degeneracy [11]. In our dots, which are prolate with a wurtzite crystal structure (long axis $\parallel$ to the unique hexagonal "c" axis), the band edge state is split into two fourfold degenerate levels, analogous to the bulk "*A-B* splitting." The net splitting is the sum of the internal crystal field and shape asymmetry components,

$$\Delta = \Delta_{\text{int}} + \Delta_{\text{asym}}(\beta, \mu, a), \tag{1}$$

where β is the ratio of effective masses of the bulk A and B bands along the c axis, a is the dot radius, and μ, the degree of ellipticity, is defined as $\mu = c/b - 1$, where c (b) is the major (minor) axis [11].

The band edge state is further split by the electron-hole exchange interaction. Since this term is proportional to the spatial overlap between the electron and hole, an enhanced exchange effect is expected in low-dimensional structures due to carrier confinement and has been confirmed in GaAs/GaAlAs quantum wells [12]. A further enhancement is predicted in QDs due to the three-dimensional confinement of the electron and hole [13]. The exchange Hamiltonian in CdSe is [14]

$$\hat{H}_{\text{exch}} = -\frac{2}{3}\varepsilon_{\text{exch}}(a_0)^3\delta(\mathbf{r}_e - \mathbf{r}_h)(\hat{\boldsymbol{\sigma}} \cdot \hat{\mathbf{J}}), \tag{2}$$

where $\hat{\boldsymbol{\sigma}}$ is the electron Pauli spin 1/2 matrix, $\hat{\mathbf{J}}$ is the hole spin 3/2 matrix, a_0 is the lattice constant, and $\varepsilon_{\text{exch}}$ is the exchange strength constant (~320 meV in CdSe). Equation (2) mixes the electron and hole spin states, and in bulk CdSe splits the fourfold degenerate A exciton into an optically active singlet and passive triplet by $\hbar\omega_{ST} \simeq 0.13$ meV [15].

For CdSe QDs, we include the anisotropy [Eq. (1)] and exchange terms [Eq. (2)] within the framework of perturbation theory. The initially eightfold degenerate band edge exciton ($1S_{3/2}1S_e$) is split into five states labeled by the total exciton angular momentum projection, $F_m = m_e + m_j$, where $m_{e(j)}$ is the electron (hole) spin projection. Their energies can be expressed in terms of Δ

 0031-9007/95/75(20)/3728(4)$06.00

and the size dependent exchange contribution

$$\eta = (a_B/a)^3 \hbar\omega_{ST}\chi(\beta), \quad (3)$$

where $\chi(\beta)$ is a dimensionless function which equals 0.78 in CdSe.

The order of the levels in spherical dots is indicated in Fig. 1(a). These states can be classified into two groups which converge to the bulk A and B excitons: $F_m = \pm 2, \pm 1^L$ and $F_m = 0^L, \pm 1^U, 0^U$, where the superscripts U and L distinguish upper and lower states with the same angular momentum projection. Figure 1(b) shows that the crystallite shape influences the band edge structure. For example, with $\mu = 0.3$ and $\beta = 0.28$ the levels cross, and the lowest state is either the ± 2 or 0^L level, depending on the radius. Transmission electron microscope (TEM) measurements on our samples indicate that the ellipticity ranges between 0.0 and 0.3, increasing with size [5]. In this case we obtain a band edge structure which is nearly identical to that for spherical dots [Fig. 1(c)] [16]. In general, the states fan out with decreasing size due to enhancement of the exchange term. The calculated exchange splitting between the ± 2 and $\pm 1^L$ states in the smallest dots ($\sim$12.5 meV) is 2 orders of magnitude larger than the corresponding bulk value ($\sim$0.13 meV). A similar enhancement has been suggested in porous silicon [17]. The oscillator strengths of the optically active levels are also strongly modified by the exchange term and change dramatically with size [Fig. 1(d)]. Both the ± 2 and 0^L levels are optically passive within the electric dipole approximation.

We find strong evidence for this band edge structure in our photoluminescence results. We study CdSe quantum dots prepared by an organometallic synthesis which yields highly monodisperse (<4% rms) wurtzite crystallites with diameters tunable from $\sim$15 to $\sim$115 Å [5]. Excitation on the red edge of the sample absorption reduces residual sample inhomogeneities by optically selecting the "largest" crystallites in the distribution. In the resulting fluorescence line narrowing (FLN) [6] spectrum, a well resolved longitudinal optical (LO) phonon progression is observed. FLN spectra for a series of sizes spanning the strong confinement regime ($a \ll a_B$) are shown in Fig. 2(a). The Stokes shift between the excitation energy and the peak of the zero LO phonon line (ZPL) is strongly size dependent, ranging from $\sim$20 to $\sim$1 meV in this size series. According to the predicted band edge structure [Fig. 1(c)], excitation on the red edge of the absorption spectrum probes the lowest optically active level ($\pm 1^L$). The luminescence is then Stokes shifted due to efficient relaxation via acoustic phonon emission to the band edge ± 2 state. In Fig. 2(b) the data are compared with the calculated size dependent splitting between the $\pm 1^L$ and band edge ± 2 states. We obtain good agreement with no adjustable parameters using literature values: a_B = 56 Å [3], $\hbar\omega_{ST}$ = 0.13 meV [15] and β = 0.28 [4]. In the smallest crystallites, however, the exchange splitting

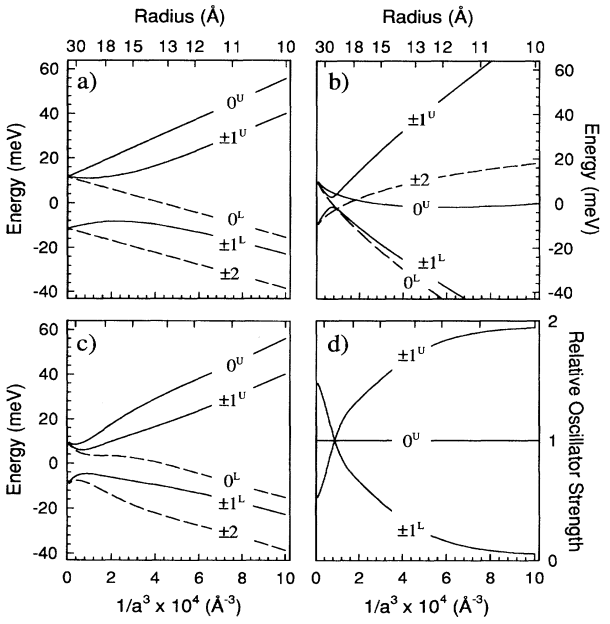

FIG. 1. Calculated band edge exciton structure vs $1/a^3$ in CdSe QDs for various shapes: (a) spherical ($\mu = 0$), (b) prolate ($\mu = 0.3$), and (c) a size dependent ellipticity consistent with TEM data. Dashed (solid) lines indicate optically passive (active) levels. (d) Oscillator strengths vs $1/a^3$ for the optically active states in (c), relative to the 0^U level.

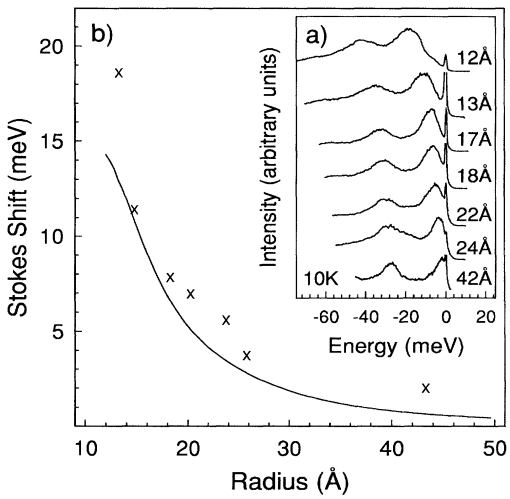

FIG. 2. (a) Normalized FLN spectra for CdSe QDs between 12 and 42 Å in radius. Mean radii are determined from TEM measurements. A 10 Hz Q-switched Nd:YAG/dye laser system ~7 ns pulses) serves as the excitation source, followed by ns time-gated, multichannel detection. A small amount of the pump laser is included for reference in each spectrum and set to zero energy for comparison. (b) Size dependence of the Stokes shift (×) between the pump position and the peak of the ZPL, extracted from the FLN spectra. The solid line is the calculated size-dependent splitting between the ± 2 and $\pm 1^L$ states from Fig. 1(c).

underestimates the observed FLN Stokes shift. This discrepancy may be due to an additional vibrational component since exciton-acoustic phonon coupling is predicted to scale as $1/a^2$ [18], which is consistent with recent data of Mittleman *et al.* [19].

The presence of an optically passive band edge state strongly affects the dynamics of electron-hole recombination. However, in bulk CdSe, where the exchange splitting is only 0.13 meV, Boltzmann factors inhibit the observation of the "dark exciton." Even at the lowest temperatures when thermal effects can be ignored, spin relaxation mechanisms mediated by the spin-orbit interaction remain highly efficient in the bulk. These terms, which mix electron spin up and down states having opposite parity, are negligible in small dots, where the closest opposite parity electron level ($1P$) is hundreds of meV above the lowest state ($1S$) [3]. Therefore, we expect dark exciton effects in small CdSe dots, where the spacing between the band edge ± 2 and lowest optically allowed $\pm 1^L$ states is large relative to kT. In Fig. 3(a) we show magnetic field dependent luminescence decays for 12 Å radius crystallites between 0 and 10 T at 1.7 K. Since the transition dipole of the $\pm 1^L$ state is $\perp$ to the c axis, these decays were obtained by exciting the sample far to the blue of the first absorption maximum to avoid artifacts associated with orientational selection in the excitation process. The emission should come primarily from the ± 2 state, as thermalization processes are highly efficient, relative to the radiative rates. The long μs emission at zero field is consistent with recombination from this weakly emitting state. With increasing magnetic field, the luminescence lifetime decreases and, as the quantum yield remains essentially constant, we interpret this as an enhancement of the radiative rate.

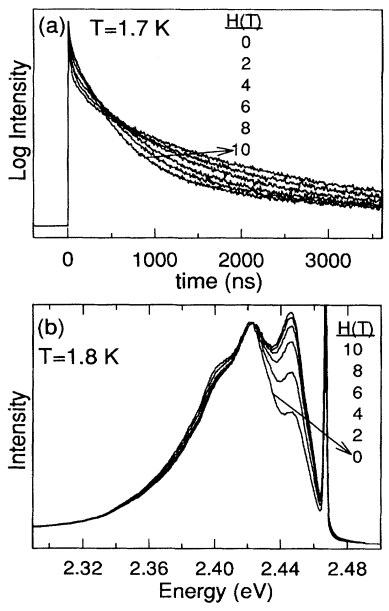

FIG. 3. Magnetic field dependence of (a) emission decays recorded at the peak of the luminescence (2.436 eV) with a pump energy of 2.736 eV, and (b) FLN spectra excited at the band edge (2.467 eV) for 12 Å radius dots and normalized to their one phonon line. A small amount of the excitation laser is included to mark the pump position. Experiments were carried out in the Faraday geometry ($\vec{H} \parallel \vec{k}$).

Since these dots are significantly smaller than the characteristic magnetic length (~115 Å at 10 T), this enhancement is not a result of Landau levels as seen in the bulk and in quantum wells. In those systems the field can enhance the oscillator strength, and consequently the radiative rate, by shrinking the excitonic wave function [20]. Within the strong confinement regime of QDs, however, the spatial extent of the carriers is determined by the dot dimensions, and the interaction with the magnetic field is well described as a molecular Zeeman effect. The field influences the mechanism of recombination primarily by mixing the various excitonic spin states [9]. Since the c axes of the crystallites in our samples are randomly oriented, the ± 2 and $\pm 1^{L,U}$ states are mixed in dots whose c axis is not aligned with the field. The admixture $|A|^2$ of the closest optically active level $\pm 1^L$ in the ± 2 state can be calculated in second order perturbation theory,

$$|A|^2 = \frac{\mu_B^2[g_e(1+\kappa) - 3g_h]^2 s(\kappa)}{3\Delta^2[2s(\kappa) - 4 + \kappa]} H^2 \sin^2(\theta), \quad (4)$$

where $g_{e(h)}$ is the electron (hole) g factor, μ_B is the Bohr magneton, $\kappa = \Delta/2\eta$, $s(\kappa) = \sqrt{3 + (1-\kappa)^2}$, H is the magnetic field, and θ is the angle between the c axis and the field for a given dot. As a result of mixing, the ± 2 state gains oscillator strength from the optically active $\pm 1^{L,U}$ states, explaining the observed decrease in radiative lifetime with increasing magnetic field.

The magnetic field dependence of the luminescence decays can be reproduced using 3-level kinetics [Fig. 4(a)]. In this model the emitting states include the $\pm 1^L$ and ± 2 levels with corresponding radiative rates $\gamma_1(\theta, H)$ and $\gamma_2(\theta, H)$. The thermalization rate γ_{th} is determined independently from picosecond time resolved measurements. Measured decays at 0 and 10 T are shown in Fig. 4(b). The decay at zero field is multiexponential, presumably due to sample inhomogeneities. To simulate this, we use three 3-level systems, each having a different value of γ_2, representing a class of dots within the inhomogeneous distribution. These 3-level systems are then weighted to reproduce the zero field decay [Fig. 4(c)]. With the zero field values of γ_1 and γ_2 fixed, their field and angle dependence [$\gamma_1(\theta, H)$, $\gamma_2(\theta, H)$] is determined with Eq. (4). The field dependent decay is then calculated, averaging over all angles to account for the random orientation of crystallite c axes. The simulated decay at 10 T [Fig. 4(c)], using the bulk value for $g_e = 0.78$ and the calculated values Δ (19.4 meV) and η (10.3 meV) for 12 Å radius dots, is in good agreement with experiment. The hole g factor is treated as a fitting parameter since

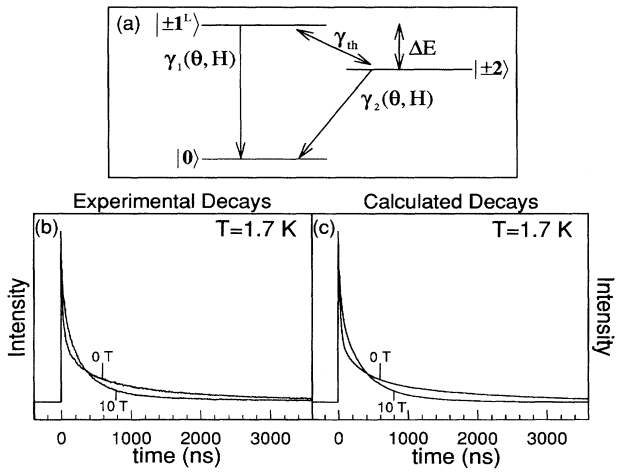

FIG. 4. (a) Three-level model used to reproduce the magnetic field dependence of the emission decays. ΔE is the splitting between the $\pm 1^L$ and ± 2 states (12.5 meV for 12 Å radius dots). $\gamma_1(\theta, H)$ and $\gamma_2(\theta, H)$ are the field and angle dependent radiative rates of the $\pm 1^L$ and ± 2 states in a given dot. γ_{th} accounts for the radiationless decay from the $\pm 1^L$ to the ± 2 state. Repopulation of the $\pm 1^L$ state is determined by microscopic reversibility. (b) Measured emission decays at 0 and 10 T for 12 Å radius dots. (c) Calculated luminescence decays based on the 3-level model. The zero field decay is simulated with three weighted 3-level systems having different values of γ_2 (0.033, 0.0033, 0.00056 ns^{-1}) and corresponding weighting factors (1, 3.8, 15.3). γ_1 (0.1 ns^{-1}) and γ_{th} (0.026 ps^{-1}) are the same in all three systems.

reliable values are not available. We use $g_h = -0.96$, consistent with theoretical estimates for this parameter.

The vibronic spectrum of the CdSe QDs is also strongly influenced by the field. Magnetic field dependent FLN spectra for 12 Å radius dots between 0 and 10 T at 1.7 K are shown in Fig. 3(b). Each spectrum is normalized to the one phonon lines for clarity. In isolation the ± 2 state would have an infinite lifetime since the photon cannot carry an angular momentum of 2 within the electric dipole approximation. However, the dark exciton can recombine via a LO phonon assisted, momentum-conserving transition [17]. Spherical LO phonons with an orbital angular momentum of 1 or 2 are expected to participate in these transitions; the selection rules determined by the coupling mechanism [11,21]. Consequently, at zero field, the higher LO phonon lines are strongly enhanced relative to the ZPL. With increasing magnetic field, the ± 2 level gains optically active $\pm 1^{L,U}$ character, diminishing the need for LO phonon assisted recombination. This explains the dramatic increase in the intensity of the ZPL, relative to the higher LO phonon replicas with increasing field.

While surface effects previously invoked to explain the photophysical behavior of CdSe QDs may still play a role, especially via nonradiative processes, the energetics and dynamics of the band edge emission can be quantitatively understood in terms of the intrinsic band edge exciton structure. The electron-hole exchange interaction and anisotropy terms split the eightfold degenerate bulk band edge exciton into five levels, labeled by the total angular momentum projection F_m. Exciton thermalization into a dipole forbidden state with $F_m = \pm 2$ resolves the issue of the long band edge luminescence lifetimes. The magnetic field dependence of the emission decays and LO phonon structure confirms the presence of this dark excitonic state and reveals its luminescence properties.

M. N. and D. J. N. benefited from AT&T and NSF fellowships, respectively. M. G. B. thanks the Lucille and David Packard Foundation and the Alfred P. Sloan Foundation for fellowships. This work was funded in part by the NSF-MRSEC program (DMR-94-00034) and by NSF (DMR-91-57491).

[1] Al. L. Efros and A. L. Efros, Sov. Phys. Semicond. **16**, 772 (1982).
[2] L. E. Brus, J. Chem. Phys. **80**, 4403 (1984).
[3] A. I. Ekimov *et al.*, J. Opt. Soc. Am. B **10**, 100 (1993).
[4] D. J. Norris, A. Sacra, C. B. Murray, and M. G. Bawendi, Phys. Rev. Lett. **72**, 2612 (1994); D. J. Norris and M. G. Bawendi (to be published).
[5] C. B. Murray, D. J. Norris, and M. G. Bawendi, J. Am. Chem. Soc. **11**, 8706 (1993).
[6] M. G. Bawendi, P. J. Carroll, W. L. Wilson, and L. E. Brus, J. Chem. Phys. **96**, 946 (1992); M. Nirmal, C. B. Murray, and M. G. Bawendi, Phys. Rev. B **50**, 2293 (1994).
[7] C. H. Henry and K. Nassau, Phys. Rev. B **1**, 1628 (1970).
[8] M. O'Neil, J. Marohn, and G. McLendon, J. Phys. Chem. **94**, 4356 (1990); A. Hasselbarth, A. Eychmuller, and H. Weller, Chem. Phys. Lett. **203**, 271 (1993).
[9] S. Nomura, Y. Segawa, and T. Kobayashi, Phys. Rev. B **49**, 13 571 (1994).
[10] M. Chamarro, C. Gourdon, P. Lavallard, and A. I. Ekimov, Jpn. J. Appl. Phys. Suppl. **34-1**, 12 (1995).
[11] Al. L. Efros and A. V. Rodina, Phys. Rev. B **47**, 10 005 (1993); Al. L. Efros, Phys. Rev. B **46**, 7448 (1992).
[12] M. Potemski, J. C. Maan, A. Fasolino, K. Ploog, and G. Weimann, Surf. Sci. **229**, 151 (1990).
[13] T. Takagahara, Phys. Rev. B **47**, 4569 (1993).
[14] G. L. Bir and G. E. Pikus, *Symmetry and Strain-Induced Effects in Semiconductors* (Wiley, New York, 1975).
[15] V. P. Kochereshko, G. V. Mikhailov, and I. N. Ural'tsev, Sov. Phys. Solid State **25**, 439 (1983).
[16] Using TEM data, we fit the size-dependent ellipticity by a polynomial.
[17] P. D. J. Calcott *et al.*, J. Phys. Condens. Matter **5**, L91 (1993).
[18] S. Nomura and T. Kobayashi, Solid State Commun. **82**, 335 (1992).
[19] D. M. Mittleman *et al.*, Phys. Rev. B **49**, 14 435 (1994).
[20] J. E. Zucker, E. Isaacs, D. Heiman, A. Pinczuk, and D. S. Chemla, Surf. Sci. **196**, 563 (1988).
[21] M. C. Klein, F. Hache, D. Ricard, and C. Flytzanis, Phys. Rev. B **42**, 11 123 (1990).